Introduction of $CaCO_3$ as Electron Recombination Barrier Layer in TiO_2-Based Dye-Sensitized Solar Cell

M. Yazdanipanah, M. R. Mohammadi*

Department of Materials Science and Engineering, Sharif University of Technology, Tehran, Iran.
Received: 20 January 2025 - Accepted: 25 May 2025

Abstract

Calcium carbonate ($CaCO_3$) is an effective material for surface modification in TiO_2-based dye-sensitized solar cells (DSSCs). Its higher conduction band position compared to TiO_2 helps reduce electron recombination rates, and its elevated isoelectric point promotes increased dye adsorption. It is crucial to control the thickness of the $CaCO_3$ layer to less than 3-10 nm, as tunneling phenomena cannot occur when the insulating layer exceeds 10 nm in thickness. In this study, the $CaCO_3$ layer was deposited using the spin-coating method. Additionally, in two samples, the second $TiCl_4$ treatment was omitted during DSSC preparation to assess its impact on the photovoltaic properties. The results indicate that while the deposition of $CaCO_3$ enhances the photocurrent of the DSSCs, it simultaneously reduces the fill factor. However, applying the $TiCl_4$ treatment both before and after $CaCO_3$ deposition improves the fill factor, leading to greater efficiency compared to the untreated samples. Specifically, sample TT3CT achieved an efficiency of 7.98%, while the neat sample reached 7.58% efficiency.

Keywords: DSSC, Surface Modification, Recombination Barrier Layer, Calcium Carbonate.

1. Introduction

Traditional and non-renewable energy sources like coal, oil, and natural gas provide a significant portion of energy demands. Burning fuels releases carbon dioxide into the atmosphere, contributing to various environmental problems [1]. Therefore, renewable energy sources like wind and solar power are suitable alternatives to be used as solutions for global energy demands [2]. Converting the sunlight to electricity, directly, by photovoltaic solar cells is one of the most efficient approaches [3, 4]. Dye-sensitized solar cells (DSSCs) which were proposed in 1991 by Gratzel and O'Regan, are popular for their cost-effective fabrication and potential for flexibility in photovoltaic devices [5, 6]. The photoanode is a key component of a DSSC, composed of a nanostructured oxide semiconductor, typically TiO_2 [7]. Although TiO_2 offers many merits for this application, the electrons injected into its conduction band can be captured by oxidizing species in the electrolyte or by oxidized dye molecules. This interaction leads to a high rate of electron recombination, which results in lower current output. Simple methods, such as acid treatment or depositing blocking layers, can effectively reduce this recombination rate [10-8].
Metal oxides or carbonates such as MgO, Al_2O_3, ZnO, and $CaCO_3$ can be deposited between TiO_2 and the electrolyte, leading to a decrease in the recombination rate [9, 11, 12]. Optimizing the thickness of the blocking layer is crucial. While this layer should block recombination, it should not prevent electron injection from dye to TiO_2 [9].

*Corresponding author
Email address: mohammadi@sharif.edu

$CaCO_3$ is one of the most abundant minerals and has many desirable properties in various applications. Calcite with a rhombohedral structure and an indirect bandgap of 6.0 eV is the most stable polymorph of $CaCO_3$ [13–15]. In addition, calcite has a higher isoelectric point than anatase, therefore, it has more basicity and can absorb more dye. The enhancement of dye absorption results in more photocurrent and efficiency. K. Tehare et al [16]. deposited four blocking layer materials and found that MgO-coated and $CaCO_3$-coated TiO_2 had the highest efficiencies, increasing from 1.97% for pure TiO_2 to 6.05% and 4.25%, respectively. Lee et al [17]. enhanced the efficiency of DSSCs from 7.8% to 9.7% by depositing a 3.5 nm thick layer of $CaCO_3$ (18). Park et al. enhanced dye-sensitized solar cell efficiency by using $CaCO_3$ surface modification and nitrogen doping in TiO_2 photoanodes, achieving 7.46% and 9.03% efficiencies, respectively [11].
Our research aims to develop a cost-effective method for depositing an ultra-thin layer of $CaCO_3$ on TiO_2 and to explore replacing $CaCO_3$ with $TiCl_4$ treatment. We also investigated the photovoltaic properties of DSSCs using both methods. The goal is to compare the performance of TiO_2-based DSSCs with the $CaCO_3$ layer and assess the effects of $TiCl_4$ treatment.

2. Materials and Methods

2.1. Synthesis of TiO_2 Nanoparticles

TiO_2 nanoparticles with particle size of 15-30 nm were synthesized using a combination of solvothermal and sol-gel techniques, following a previously established procedure [19]. For this purpose, titanium tetraisopropoxide (TTIP) (97% purity, Sigma-Aldrich, UK) was used as a Ti precursor.

2.2. Preparation of Photoanode Electrodes

FTO-coated glass substrates (Solaronix, Switzerland) were washed with detergent. After rinsing with deionized water, a compact TiO_2 layer was deposited using a 0.04 M $TiCl_4$ solution and heat-treated at 450 °C for 30 minutes. TiO_2 paste was then spin-coated onto the substrate, followed by annealing at 400 °C for 2 hours. The spin-coating parameters were set to achieve a thickness of 35 µm, which was optimized in the previous work [20]. To deposit the ultra-thin layer of $CaCO_3$, solutions of $Ca(NO_3)_2$ and NaOH were prepared using a 1:1 mixture of deionized water and ethanol. Three drops of the $Ca(NO_3)_2$ and NaOH solutions were placed on the surface of the photoanodes and then spin-coated at a speed of 5000 rpm for 2 minutes each. The number of cycles for $CaCO_3$ deposition for each sample can be found in Table. 1. Next, a 0.5 cm × 0.5 cm square of the film was trimmed. A 0.5 mM dye solution (ruthenium 535-bisTBA; Solaronix, Switzerland) was prepared in ethanol, and the photoanode electrodes were immersed in this solution for 21 hours in the dark. Afterward, the dye-loaded photoanodes were rinsed with ethanol and used for photovoltaic measurements. To further characterize the formation of $CaCO_3$, the powders were synthesized by reacting $Ca(NO_3)_2$ and NaOH solutions without a TiO_2 substrate. These powders were treated using the same method employed for the $CaCO_3$ coating on TiO_2 surfaces. Sample TT underwent post-treatment with a 0.01 M $TiCl_4$ solution after the deposition of the TiO_2 nanoporous film. Similarly, samples TT1CT and TT3CT were treated using the same method, both before and after $CaCO_3$ deposition. All three samples were then annealed at 450 °C for 30 minutes in an air atmosphere after each treatment step.

Table. 1. Characteristics of $CaCO_3$-deposited on TiO_2 DSSCs.

Sample	Cycles of $CaCO_3$ deposition	Photoanode layers arrangement
TT	-	TiO_2 + $TiCl_4$ treatment
T1C	1	TiO_2 + $CaCO_3$ layer (1 Cycle)
T3C	3	TiO_2 + $CaCO_3$ layer (3 Cycles)
TT1CT	1	TiO_2 + $TiCl_4$ treatment + $CaCO_3$ layer (1 Cycle) + $TiCl_4$ treatment
TT3CT	3	TiO_2 + $TiCl_4$ treatment + $CaCO_3$ layer (3 Cycles) + $TiCl_4$ treatment

2.3. Fabrication of DSSCs

The counter electrode was prepared by drop-coating a solution of H_2PtCl_6 onto a cleaned FTO substrate with a 1 mm hole for electrolyte injection. After drying at 60°C, it underwent heat treatment at 450°C for 30 minutes.

The dye-soaked photoanode and Pt-coated counter electrode were sandwiched using Surlyn film (SX 1170-60, Solaronix, Switzerland). Finally, an iodine-based electrolyte was injected using a vacuum. Fig. 1. shows the schematic of the photoanode layers arrangement (a) sample TT, (b) samples T1C and T3C, and (c) samples TT1CT and TT3CT.

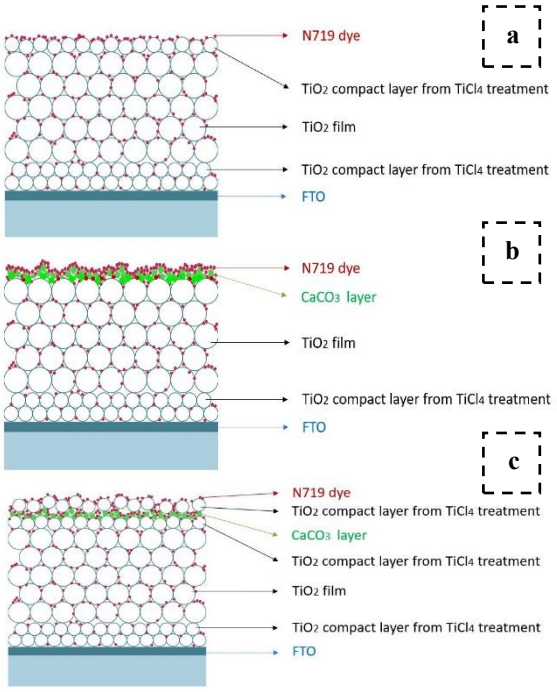

Fig. 1. Schematic of different structures of photoanode electrodes: (a) TT, (b) T1C and T3C, (c) TT1CT and TT3CT.

2.4. Characterization and Measurements

The morphology of the synthesized samples and photoanodes was examined using a Mira-III field emission scanning electron microscope (FE-SEM) from TESCAN, Czech Republic. The crystal structures of TiO_2 and $CaCO_3$ were analyzed via X-ray diffraction (XRD) with an X'pert Pro MPD diffractometer from PANalytical, Germany, over a 2θ range of 10° to 90° (Cu Kα, λ = 1.5406 Å). Thermogravimetric analysis (TGA) of $CaCO_3$ was conducted in a nitrogen atmosphere at a heating rate of 5 °C/min using a Mettler Toledo system.
The amount of dye adsorbed on the photoanodes was measured with a UV-Vis spectrophotometer (6705 JENWAY, UK) in a 0.1 M NaOH solution. Photovoltaic metrics of the DSSCs were evaluated using a Zahner CIMPA-pcs solar simulator under standard conditions (irradiance of 100 mW/cm², AM 1.5, and a scan rate of 50 mV/s).

3. Results and Discussion

3.1. Morphology and Microstructure

Fig. 2. shows the FE-SEM image of the surface of the TiO_2 nanoporous film. The image illustrates that

the TiO_2 nanoparticles range between 10-30 nm and have spherical morphology. The nanoparticles of TiO_2 have agglomerated to form TiO_2 nanoporous film. Since the $CaCO_3$ layer was ultra-thin, the FE-SEM and EDS analyses could not show the morphology of the $CaCO_3$ layer.
Therefore, to characterize the $CaCO_3$ particles, the mentioned precursors were mixed with 10 times more concentration without TiO_2 film as the substrate.

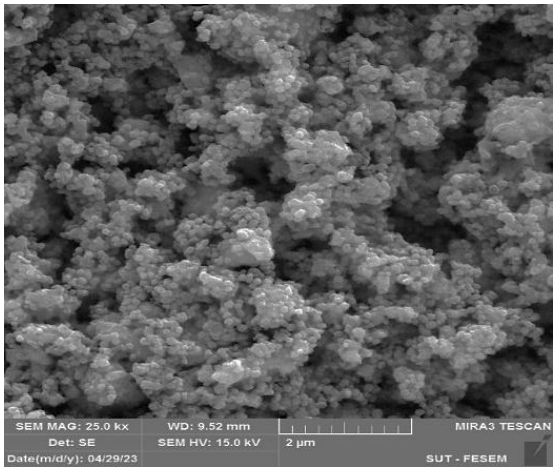

Fig. 2. FE-SEM image of TiO_2 nanoporous film.

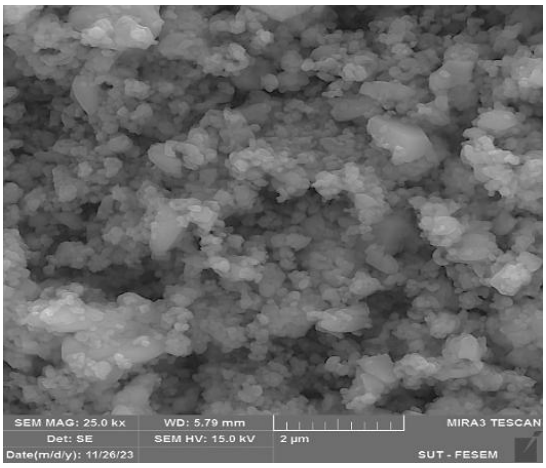

Fig. 3. FE-SEM of $CaCO_3$ particles.

Fig. 3. depicts the FE-SEM image of the $CaCO_3$, which was synthesized by this method. Second, the $CaCO_3$ layer was deposited on the surface of the TiO_2 substrate, using different spin-coating parameters and more cycles of deposition, followed by annealing at 450 °C for 30 min, just to characterize the $CaCO_3$ layer.
Fig. 4.(a) illustrates the surface of the $CaCO_3$ thick layer, and Fig. 4.(b) is related to the cross-section of the layer.
As shown in Fig. 4., $CaCO_3$ particles exhibit rhombohedral morphology with particle sizes ranging between 300-600 nm.

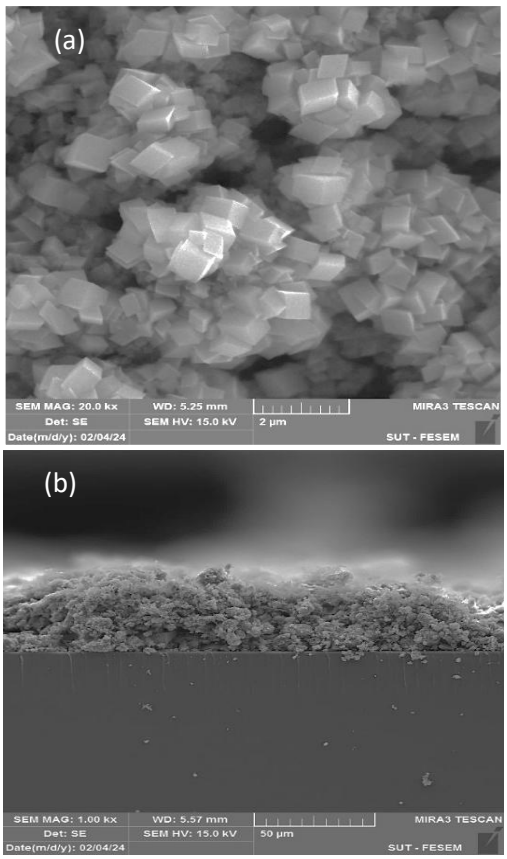

Fig. 4. FE-SEM images of the $CaCO_3$ layer on the surface of the TiO_2 nanoporous film: (a) surface view and (b) cross-sectional view.

The XRD technique was employed to analyze the crystal phase and structure of the synthesized materials. As demonstrated in Fig. 5., the pure anatase phase of TiO_2 was synthesized, and the most intense peak observed at $2\theta = 25.32°$, which matches card number 21-1272 in the JCPDS database.

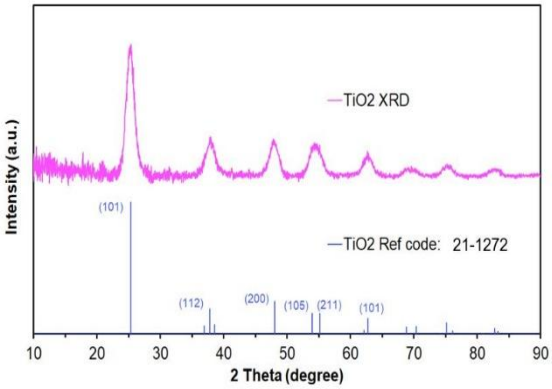

Fig. 5. XRD pattern of anatase-TiO_2 nanoparticles.

Fig. 6 shows that the calcite phase of the $CaCO_3$ was synthesized using the mentioned approach. The most intense peak appears at $2\theta = 29.39°$. All other peaks are fully aligned with the card number 05-0586 in the JCPDS database.

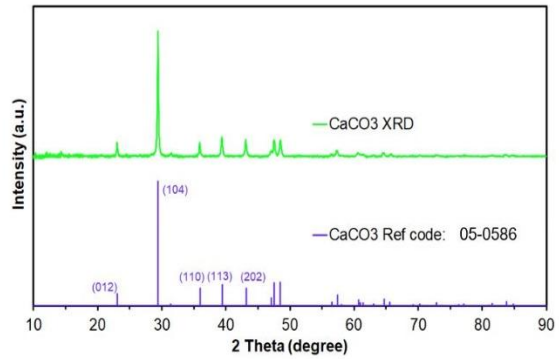

Fig. 6. XRD pattern of $CaCO_3$ particles.

The thermal behavior of $CaCO_3$ powder was investigated by thermogravimetric analysis. As exhibited in Fig. 7, the TGA curve has 3 different steps. Step 1 is related to removing water from amorphous $CaCO_3$, occurring from room temperature to approximately 250 °C.

The second step, which happens from 250 °C to 450 °C, is attributed to the loss of structural water in crystalline $CaCO_3$. The decomposition of $CaCO_3$ to CaO and CO_2 shows a significant weight loss of 44%, starting from 500 °C. Therefore, after $CaCO_3$ deposition, the annealing temperature was chosen at 450 °C to ensure structural water was removed and $CaCO_3$ was kept in the system.

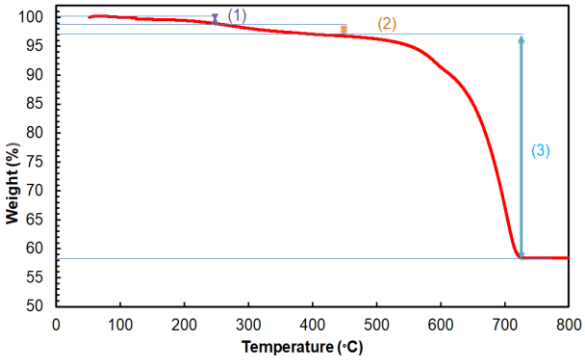

Fig. 7. TGA curve of synthesized $CaCO_3$ particles.

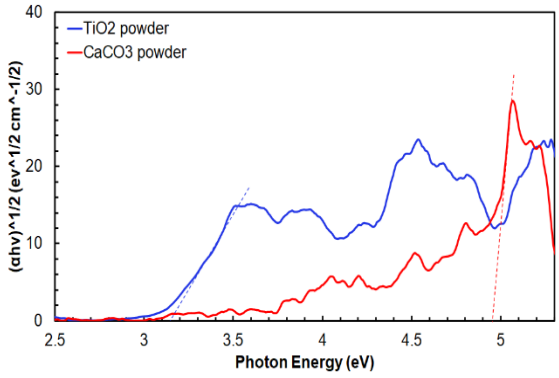

Fig. 8. Tuac plot of $CaCO_3$ and TiO_2 powders.

The optical properties of the synthesized $CaCO_3$ and TiO_2 powders were examined using diffuse reflectance spectroscopy analysis.

The band gap of $CaCO_3$ and TiO_2 powders, determined using the Tauc model, is presented in Fig. 8. The calculated band gap of TiO_2 is 3.17 eV and this is 4.95 eV for $CaCO_3$. The result shows that $CaCO_3$ can role as insulating layer on the surface of TiO_2 nanoporous film. Fig. 9. illustrates the photovoltaic properties DSSCs, highlighting parameters such as open circuit voltage (Voc), short circuit current (Jsc), power conversion efficiency (η), and fill factor (FF). These parameters are summarized in Table. 2.

Table. 2. Photovoltaic parameters of DSSCs.

Sample	Jsc (mA/cm²)	Voc (V)	FF (%)	η (%)
TT	16.28	0.74	0.63	7.58
T1C	22.20	0.70	0.46	7.14
T3C	17.53	0.70	0.43	5.27
TT1CT	15.13	0.76	0.66	7.59
TT3CT	16.64	0.75	0.64	7.98

The baseline for comparison is the pure TiO_2 DSSC (denoted as TT), which has a Jsc of 16.28 mA/cm², a Voc of 0.74 V, a fill factor of 0.63, and an overall efficiency of 7.58%. By depositing $CaCO_3$, the photocurrent of the samples increased, except for TT1CT. The enhancement in photocurrent is due to the blocking of electron recombination and enhanced dye adsorption by depositing $CaCO_3$ ultra-thin layer. Significant improvements in Jsc were observed for samples T1C and T3C; however, both Voc and fill factor decreased in these cases. Consequently, the overall efficiencies for T1C and T3C dropped to 7.14% and 5.27%, respectively. As indicated in Table 2, the series resistance increased in these samples, leading to a reduction in the fill factor from 0.63 to 0.46 for T1C and 0.43 for T3C. This decrease in fill factor is attributed to the omission of the $TiCl_4$ treatment, which typically enhances the fill factor of DSSCs by improving surface roughness and layer interaction. A comparison between the fill factors of TT1CT and TT3CT with T1C and T3C demonstrates the significant impact of $TiCl_4$ treatment on DSSCs.

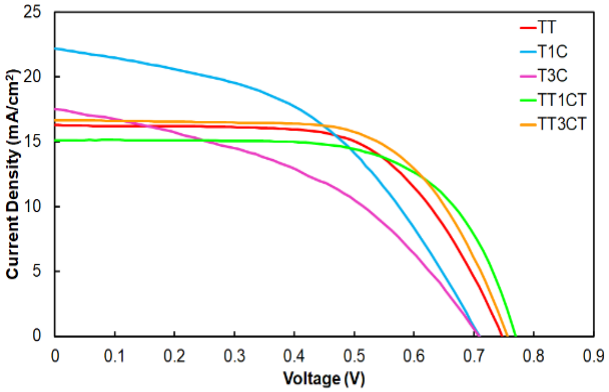

Fig. 9. J-V curves of DSSCs.

The fill factors reached 0.66 and 0.64 for TT1CT and TT3CT, respectively. Although Jsc decreased compared to T1C and T3C, the overall efficiencies of TT1CT and TT3CT were higher than those of the other samples due to their optimization of Jsc, Voc, and fill factor. TT3CT shows the best performance among other samples with an enhancement of 5% in efficiency compared to TT.

The measurement of dye absorption for TT, T1C, and T_3C, which is shown in Fig. 10. and summarized in Table. 3., indicates that the amount of absorbed dye increased with the addition of $CaCO_3$. This was expected, as $CaCO_3$ has a higher isoelectric point and can interact with the carboxylic acid groups of the dye molecules.

Specifically, the dye adsorption increased from 4.98 10^{-8} mol/cm² to 13.80 10^{-8} mol/cm² for T1C and 19.53 10^{-8} mol/cm² for T_3C.

A greater amount of dye absorption can enhance photocurrent generation by improving light harvesting within the system. However, a comparison of the results from Table. 2. and Table. 3. shows that this increase in absorption alone is insufficient for achieving greater efficiency.

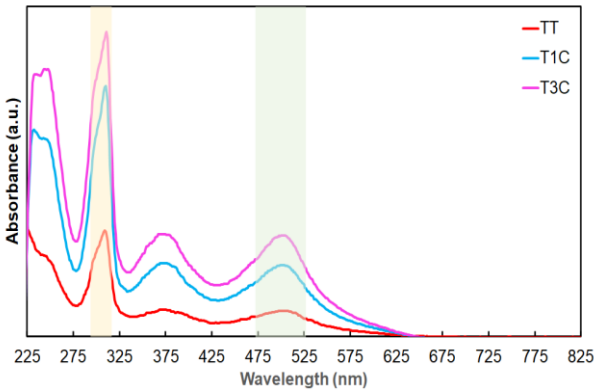

Fig. 10. UV-vis spectroscopy of photoanodes with N719 dye.

Other photovoltaic parameters, such as the fill factor, are also critical for reaching higher efficiency. For instance, T1C, despite having a significantly higher dye adsorption of 19.53 × 10^{-8} mol/cm², demonstrates a much lower efficiency of 5.78%. This suggests that omitting the $TiCl_4$ treatment negatively affects electron transport and increases resistance in the system, ultimately overshadowing the advantages of higher dye absorption.

Table. 3. The amount of dye adsorption.

Sample	Dye adsorption (mol/cm²) × 10^{-8}
TT	4.98
T1C	13.80
T3C	19.53

4. Conclusion

An ultra-thin layer of $CaCO_3$ can enhance the photocurrent of DSSCs by preventing electron recombination and increasing dye absorption. However, using $CaCO_3$ alone is not a sufficient substitute for $TiCl_4$ treatment, as omitting $TiCl_4$ results in a lower fill factor for the system. Samples that underwent both $TiCl_4$ treatment and $CaCO_3$ deposition exhibited higher photocurrent, fill factor, and overall efficiency. Nonetheless, their photocurrent was still lower than that of samples with only $CaCO_3$ deposition. Notably, sample TT3CT demonstrated a 5% increase in efficiency compared to the neat sample TT.

References

[1] Li W, Liu J, Zhao D. Mesoporous materials for energy conversion and storage devices. Nat. Rev. Mater. 2016; 4;1(6):1-7.

[2] Dambhare MV, Butey B, Moharil SV. Solar photovoltaic technology: A review of different types of solar cells and its future trends. JPCS J. Phys: Conf. Ser. 2021;1913:012053.

[3] Ellabban O, Abu-Rub H, Blaabjerg F. Renewable energy resources: Current status, future prospects and their enabling technology. Renew.Sustain Energy Rev. 2014;1;39:748-764.

[4] Nayak PK, Mahesh S, Snaith HJ, Cahen D. Photovoltaic solar cell technologies: analysing the state of the art. Nat. Rev. Mater. 2019;4(4):269-285.

[5] O'regan B, Grätzel M. A low-cost, high-efficiency solar cell based on dye-sensitized colloidal TiO_2 films. Nat. 1991;353(6346):737-740.

[6] Mariotti N, Bonomo M, Fagiolari L, Barbero N, Gerbaldi C, Bella F, Barolo C. Recent advances in eco-friendly and cost-effective materials towards sustainable dye-sensitized solar cells. Green Chem. 2020;22(21):7168-218.

[7] Golvari P, Nouri E, Mohsenzadegan N, Mohammadi MR, Martinez-Chapa SO. A single layer deposition of Li-doped mesoporous TiO_2 beads for low-cost and efficient dye-sensitized solar cells. New J Chem. 2021;45(5):2470-2477.

[8] Pascoe AR, Bourgeois L, Duffy NW, Xiang W, Cheng YB. Surface state recombination and passivation in nanocrystalline TiO_2 dye-sensitized solar cells. J. Phys. Chem. C 2013; 27;117(47):25118-26.

[9] Saxena V, Aswal DK. Surface modifications of photoanodes in dye sensitized solar cells: enhanced light harvesting and reduced recombination. Semicond. Sci. Technol. 2015; 22;30(6):064005.

[10] Sireesha P, Sun WG, Su C, Kathirvel S, Lekphet W, Akula SB, Li WR. Enhancement of power conversion efficiency of TiO_2-based dye-sensitized solar cells on various acid treatment. JNN J.Nanosci.Nanotechnol. 2017; 17(1):354-362.

[11] Park SK, Yun TK, Bae JY, Won YS. Combined embedding of N-doping and $CaCO_3$ surface modification in the TiO_2 photoelectrodes for dye-sensitized solar cells. Appl. Surf. Sci. 2013;15(285):789-794.
[12] Madhu Mohan V, Murakam K, Jonnalagadda M, Machavaram VR. Improved efficiency in dye-sensitized solar cell via surface modification of TiO2 photoelectrode by spray pyrolysis. J. Mater. Sci.Mater. Electron. 2021;32(13):18231-9.
[13] Brittain HG. Profiles of drug substances, excipients and related methodology. AP Academic Press. 2016; 26.
[14] Racca LM, Bertolino LC, Nascimento CR, de Sousa AM, Reznik LY, Yokoyama L, da Silva AL. Myristic acid as surface modifier of calcium carbonate hydrophobic nanoparticles. JNR J. Nanoparticle Res. 2019;21:1-3..
[15] Hossain FM, Murch GE, Belova IV, Turner BD. Electronic, optical and bonding properties of $CaCO_3$ calcite.Solid-State Commun. 2009;149(29-30):1201-3.
[16] Wang ZS, Yanagida M, Sayama K, Sugihara H. Electronic-insulating coating of $CaCO_3$ on TiO_2 electrode in dye-sensitized solar cells: improvement of electron lifetime and efficiency. Chem. Mater. 2006;18(12):2912-2916.
[17] Tehare KK, Navale ST, Stadler FJ, He Z, Yang H, Xiong X, Liu X, Mane RS. Enhanced DSSCs performance of TiO_2 nanostructure by surface passivation layers. Mater. Res. Bull. 2018; 99:491-495.
[18] Lee S, Kim JY, Youn SH, Park M, Hong KS, Jung HS, Lee JK, Shin H. Preparation of a nanoporous CaCO3-coated TiO2 electrode and its application to a dye-sensitized solar cell. Langmuir. 2007; 23(23):11907-10.
[19] Gharavi PM, Mohammadi MR. The improvement of light scattering of dye-sensitized solar cells aided by a new dandelion-like TiO_2 nanostructures. Sol. Energy Mater. Sol. Cells. 2015; 137:113-123.
[20] Khazaei M, Mohammadi MR, Li Y. Dye-sensitized solar cells based on anatase-and brookite-TiO_2: enhancing performance through optimization of phase composition, morphology and device architecture. Nanotechnology. 2024; 35(38):385602.